DOI: 10.1002/ejic.200500432

Amino-phosphanes in Rh^{I}-Catalyzed Hydroformylation: Hemilabile Behavior of P,N Ligands under High CO Pressure and Catalytic Properties

Jacques Andrieu,*[a] Jean-Michel Camus,[a] Philippe Richard,[a] Rinaldo Poli,[a,b] Luca Gonsalvi,[c] Francesco Vizza,[c] and Maurizio Peruzzini*[c]

Keywords: Rhodium / Amino-phosphane ligands / Hemilability / Hydroformylation catalysis

The catalytic properties of rhodium complexes containing the α-, β-, or γ-amino-phosphane ligands $Ph_2PCH_2NEt_2$ (**α-P,N-1**), $Ph_2PCH(Ar)NHPh$ [**α-P,N-2**; Ar = η^6(*o*-C_6H_4Cl)$Cr(CO)_3$], $Ph_2PCH_2NPh_2$ (**α-P,N-3**), $Ph_2PCH_2CH(Ph)NHPh$ (**β-P,N**), Ph_2PCH_2(*o*-C_6H_4–NMe_2) (**γ-P,N-1**), Ph_2PCH(*o*-C_6H_4–CH_2NHPh) (**γ-P,N-2**), and the α,β-diamino-phosphane ligand $Et_2NCH_2P(Ph)CH_2CH(Ph)NHPh$ (**α,β-N,P,N**), in styrene hydroformylation have been examined. The results show that the activity increases when the number of backbone carbon atoms linking P and N decreases from 3 to 1. IR and ^{31}P HPNMR studies in solution show that all P,N ligands adopt exclusively a κ^1-*P* coordination mode in rhodium chloride carbonyl complexes under high CO pressure. In the solid state a κ^1-*P*-α-amino-phosphane coordination has been ascertained by X-ray methods in *trans*-[RhCl(CO)(**γ-P,N-1**)$_2$]. In contrast, an equilibrium between the κ^2-*P,N* and κ^1-*P*-coordination modes has been observed as a function of the CO pressure for the complex containing the **β-P,N** ligand. The basicity of the dangling amino group also plays an important role on the catalytic activity and a mechanism involving the nitrogen function in the catalytic cycle is proposed.

Introduction

Bifunctional P,N ligands are being intensively investigated because they present advantages compared to common trialkyl phosphanes in the catalytic applications of their corresponding Pd, Ni, Ru, and Ir complexes.[1–8] These ligands can be either κ^1-*P* or κ^2-*P,N* coordinated and each coordination mode can modify the catalytic properties. For example, the chelating coordination mode enhances the nucleophilic character of the metal center and subsequently promotes hydrogen oxidative addition.[7,9,10] A comparative study between α- and β-amino-phosphanes in rhodium-catalyzed hydroformylation has led to the proposal that a bidentate coordination mode accelerates aldehyde reductive elimination from RhH_2(acyl)(P,N).[11] The authors conclude that uncoordinated amino functions do not act as bases. In contrast, the dangling amine function in a Pd^{II}-coordinated κ^1-*P*-pyridinylphosphane acts as a "proton messenger" in catalytic alkyne methoxycarbonylation.[1] In another study of rhodium-catalyzed hydroformylation, it was shown that the P,N,P type, $Ph_2PCH_2N(Ar)CH_2PPh_2$, ligand is much more active than its analogous $Ph_2P(CH_2)_3$-PPh_2. However, a rationalization for the latter observation was not proposed.[12]

One of the key questions related to the use of bifunctional ligands, particularly those associating soft and hard donor atoms, is whether there is reversible association/dissociation of one labile function during the catalytic cycle (*hemilability* concept). In our laboratory, we have developed different pathways to chiral α- or β-P,N and mixed α,β- and β,γ-N,P,N ligands and their coordination properties have been explored in palladium(II) and rhodium(I) complexes.[13–16] Particularly, we have reported that β-P,N ligands adopt a chelating mode whereas α-P,N ligands are only P-coordinated in Cu^{I} or in Rh^{I} complexes.[17,18] Separate work has shown that β-P,N ligands in Rh^{I} complexes can adopt a monodentate κ^1-P-[19] or a κ^2-*P,N*-coordination mode.[15,20] Nevertheless, no direct evidence for a hemilabile character has been reported so far for β-P,N ligands in Rh^{I} complexes. This behavior was only suggested for a few cationic complexes of type $[Rh(COD)(\beta\text{-P,N})]^+$ in order to rationalize a rapid fluxional process.[21] Nor is it known whether the coordinated N donor in these Rh^{I} complexes and in related complexes with γ-amino-phosphanes is displaced by CO under catalytic conditions. A hemilabile behavior for related chiral P,N ligands could explain the low enantioselectivities observed in asymmetric Rh-catalyzed hydroformylation.[22,23] On the other hand, an optically pure Ru^{II} β-amino-phosphane complex led to higher *ee* for

[a] Laboratoire de Synthèse et Electrosynthèse Organométalliques, UMR 5188 CNRS, Université de Bourgogne, Faculté des Sciences Mirande,
9 avenue Alain Savary, 21078 Dijon, France
[b] Laboratoire de Chimie de Coordination, UPR CNRS 8241, 205 route de Narbonne, 31077 Toulouse Cedex, France
[c] ICCOM-CNR, Istituto di Chimica dei Composti Organometallici, Area di Ricerca CNR di Firenze,
10 Via Madonna del Piano, 50019 Sesto Fiorentino (Firenze), Italy
E-mail: Jacques.Andrieu@u-bourgogne.fr

the asymmetric reduction of ketones, whereas a related Ru-γ-amino-phosphane complex led to the same product in racemic form.[6]

We now wish to provide new information on the effect of a dangling vs. a coordinated nitrogen function of chiral P,N ligands in rhodium hydroformylation catalysis, thus helping to clarify a few previously obscure points.[11,12] Consequently, we have (i) investigated the mono- or bidentate coordination mode of P,N ligands in rhodium complexes under CO pressure by ^{31}P HPNMR and IR spectroscopy, (ii) examined the catalytic properties of various Rh^{I}–P,N complexes in styrene hydroformylation in order to establish a relation with the coordination modes, and (iii) evaluated the effect of the N basicity in P,N ligands on the formation and properties of the catalytic species.

Results

Coordination, IR, and $^{31}P\{^{1}H\}$ HPNMR Studies of Amino-Phosphanes in Rh^{I} Complexes

We first examined whether the nitrogen donor in different P,N ligands (see Scheme 1) is coordinated under catalytic conditions. This investigation completes our recent studies on the Rh^{I} coordination chemistry of P,N ligands.[15,18] Indeed, we have already reported that complex RhCl(COD)(**α-P,N-2**) (complex **1**) adopts a κ^1-*P* coordination mode both in the solid state and in solution and that an analogous monodentate coordination mode is also adopted in the dicarbonyl complex $RhCl(CO)_2$(**α-P,N-2**) (**IIα**, see Scheme 2).[18] The latter was obtained by ligand exchange from RhCl(COD)(**α-P,N-2**) (COD = 1,5-cyclooctadiene) under high CO pressure. Lowering the CO pressure did not result in the formation of a κ^2-*P,N* mononuclear product (**Iα**), but rather induces a ligand redistribution to yield $RhCl(CO)$(**α-P,N-2**)$_2$ (**IIIα**) where both α-P,N ligands are once again κ^1-*P* coordinated.

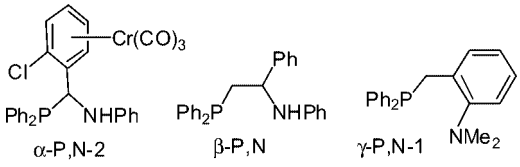

Scheme 1.

The behavior of Rh^{I} complexes containing the **β-P,N** and **γ-P,N-1** ligands was first studied by IR in CH_2Cl_2 solution under CO (see Figure 1). Irrespective of the amino-phosphane, the IR spectrum shows two absorption bands at 2092 and at 2010 cm^{-1}, corresponding to the type-**II** dicarbonyl rhodium complex (named **IIγ** and **IIβ**, with the **γ-P,N-1** and **β-P,N** ligands, respectively) where the amino-phosphane is κ^1-*P* coordinated. However, the IR spectrum of **IIβ** shows an additional absorption band at 1986 cm^{-1} corresponding to **Iβ**, as will be discussed in detail below.

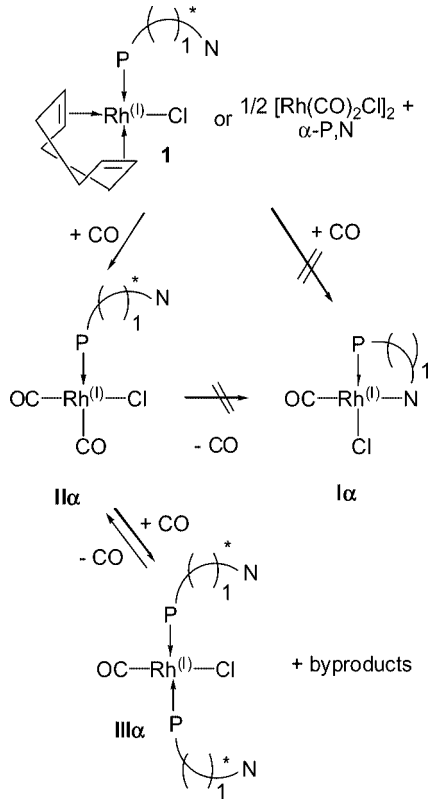

Scheme 2.

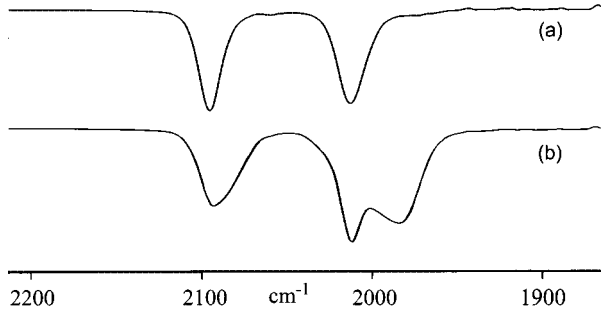

Figure 1. IR spectra of $[Rh(CO)_2Cl]_2$ + P,N ligand mixtures in 1:2 ratio prepared in CH_2Cl_2 under CO at room temperature, (a) with the **γ-P,N-1** ligand and (b) with the **β-P,N** ligand.

We then carried out $^{31}P\{^{1}H\}$ high pressure (HP) NMR studies for both dicarbonyl rhodium complexes **IIγ** and **IIβ** in order to confirm the IR results and to obtain additional information on their stability. When a solution of [RhCl(COD)(**γ-P,N-1**)] (complex **2**) was pressurized with CO, its doublet resonance at δ = 29.5 ppm [$^{1}J_{(Rh,P)}$ = 150 Hz] was replaced by a new one at δ = 26.9 ppm [$^{1}J_{(Rh,P)}$ = 126 Hz] (see Figure 2). The presence of a single complex is consistent with the IR data. After depressurization, complex **IIγ** evolved to complex **IIIγ**, [doublet at δ = 30.5 ppm with $^{1}J_{(Rh,P)}$ = 126 Hz] which became the only detectable product after flushing the solution for a few minutes with a dinitrogen stream (see Figure 2). The assignment of this

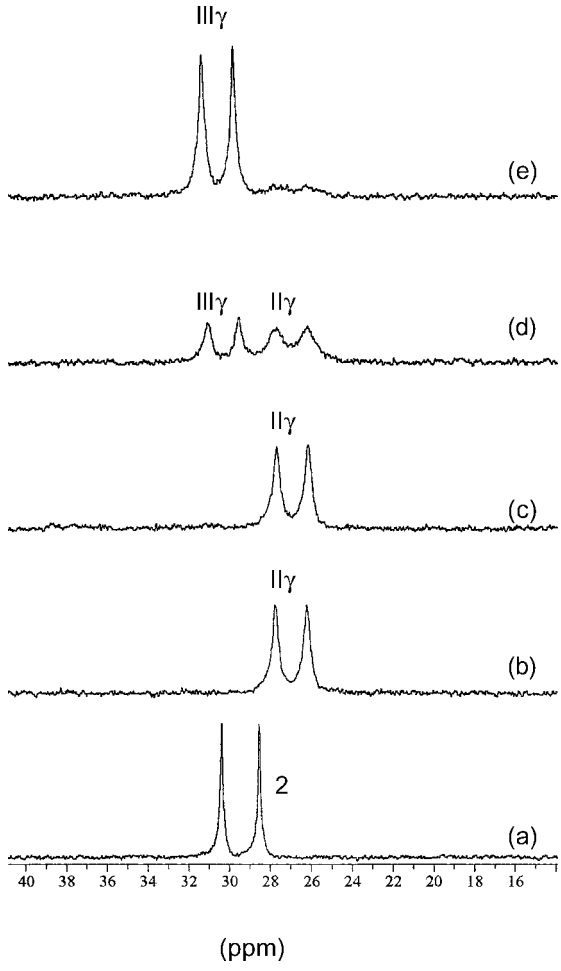

Figure 2. $^{31}P\{^{1}H\}$ HPNMR spectra under CO pressure for complex **2** in $CDCl_3$ solution. (a) Under N_2, (b) under CO, (c) under 20 bar of CO, (d) after depressurization, (e) solution after flushing 5 min with N_2.

signal to the monocarbonyl-bis-amino-phosphane rhodium complex **IIIγ** was confirmed by an X-ray structure analysis. Crystals of complex **IIIγ** (see Figure 3) were obtained upon attempting to crystallize complex **IIγ**, and their redissolution in $CDCl_3$ led to a ^{31}P NMR spectrum identical to spectrum (e) in Figure 2. Therefore, the final product of the NMR experiment in Figure 2 is unambiguously identified as a monocarbonyl-bis-amino-phosphane rhodium complex.

The evolution of **IIγ** to **IIIγ** must be accompanied by the formation of undefined organometallic CO-free by-products, as described previously for the analogous evolution of the **α-P,N-2** rhodium complex.[18] The ν_{CO} value at 1974 cm^{-1} for **IIIγ** is close to that found for $[RhCl(CO)(PPh_3)_2]$ (1965 cm^{-1}),[24] thus suggesting similar electronic properties for the **γ-P,N-1** ligand and triphenylphosphane. Table 1 shows quite typical geometrical features and metric parameters for a complex of type $RhCl(CO)L_2$ (i.e.: L = trialkyl-, dialkyl-*N*-pyrrolidinyl-, or α-amino-phosphanes), namely a nearly ideal square-planar geometry around the rhodium atom with mutually *trans* phosphorus atoms.[18,24]

Table 1. Selected bond lengths [Å] and angles [deg] for **IIIγ**.

Rh–P	2.3199(7)
Rh–C(1)	1.800(4)
Rh–Cl	2.3681(9)
C(1)–O	1.161(5)
P–Rh–P#	172.83(3)
C(1)–Rh–P	93.584(17)
C(1)–Rh–Cl	180.0
P–Rh–Cl	86.416(17)
O–C(1)–Rh	180.0

Symmetry transformations used to generate equivalent atoms: # $-x, y, -z + 1/2$

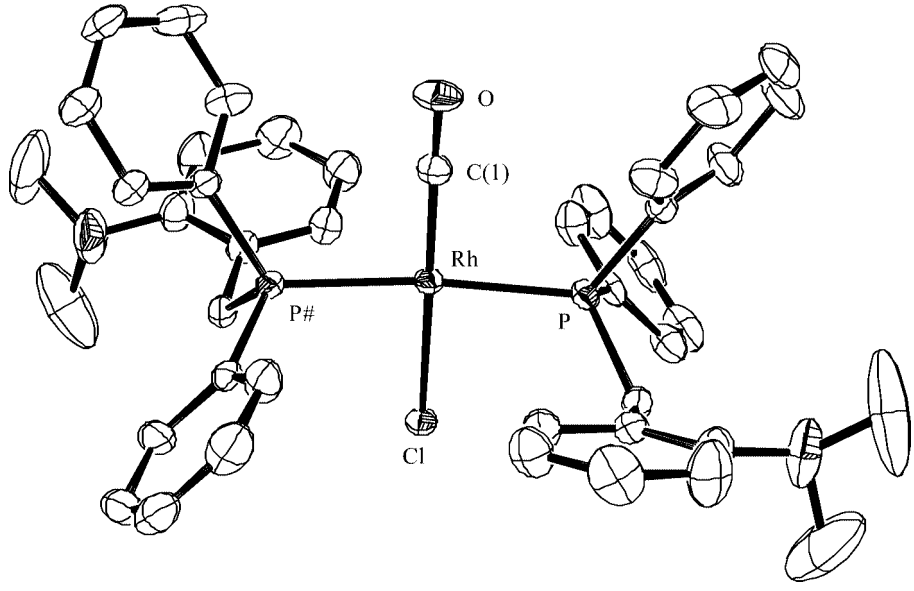

Figure 3. ORTEP view of complex **IIIγ**. Thermal ellipsoids are drawn at the 50% probability level. H atoms are omitted for clarity.

Worth noting in the structure is that the γ-P,N ligand does not chelate the rhodium center, contrary to what has been reported for a variety of Cu, Ru, Pd, and Rh complexes with the related ligands $Ph_2PCH_2[o\text{-}C_6H_4\text{–}N(Me)\text{-}CH_2CH_2OH]$, $Ph_2P(o\text{-}C_6H_4\text{–}CH_2NHtBu)$, $Ph_2P(o\text{-}C_6H_4\text{–}CH_2NMe_2)$, and $PhP[o\text{-}C_6H_4\text{–}CH(Me)NMe_2]_2$, respectively.[25–28] All the above results show that the α- and γ-P,N ligands adopt the same coordination mode in rhodium chloride complexes and undergo an identical ligand redistribution process (see Scheme 3).

A different situation was observed in the case of rhodium complexes containing the **β-P,N** ligand. Indeed, as mentioned above, the infrared spectrum recorded under CO shows an absorption band at 1986 cm^{-1} (see Figure 1), in addition to the two carbonyl bands at 2092 and 2011 cm^{-1} attributed to **IIβ**. This band corresponds to complex **Iβ**, as proven by its independent preparation and characterization (see Exp. Sect.). The simultaneous presence of **Iβ** and **IIβ** suggests the existence of an equilibrium between the two complexes under CO. This equilibrium could be followed by running two dedicated $^{31}P\{^1H\}$ NMR experiments.

The first experiment was carried out under CO on a $CDCl_3$ solution containing $[RhCl(CO)_2]_2$ and the **β-P,N** ligand. The $^{31}P\{^1H\}$ NMR spectrum showed two doublets at δ = 56 ppm [$^1J_{(Rh,P)}$ = 168 Hz] and at δ = 21 ppm [$^1J_{(Rh,P)}$ = 122 Hz] in ca. 1:2.5 ratio. The signal at δ = 56 ppm corresponds to complex **Iβ**, as verified by comparison with an authentic sample. Following the evidence provided by the IR spectrum (vide supra), the second resonance is assigned to the dicarbonyl complex **IIβ**. The second experiment was carried out under a higher CO pressure (20 bar) on a $CDCl_3$ solution containing complex [RhCl(COD)(**β-P,N**)], **3**, readily formed in situ from $[RhCl(COD)]_2$ and **β-P,N**. In this case, we observed only the doublet related to complex

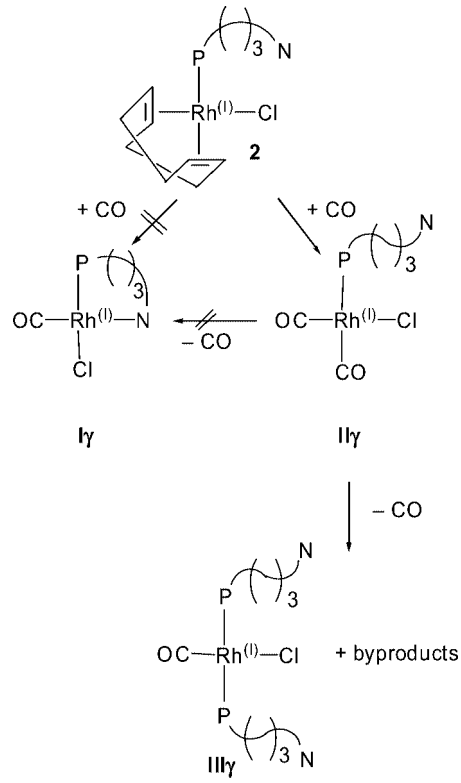

Scheme 3.

IIβ and no signal at δ = 56 ppm [see spectra (a) and (b), Figure 4].

After keeping the NMR solution pressurized with CO for 14 h, it was surprising to observe a new broad doublet at δ = 19 ppm [with $^1J_{(Rh,P)}$ = 168 Hz], named **II′β**, [see spectrum (c), Figure 4]. Tentatively, we attribute this broad

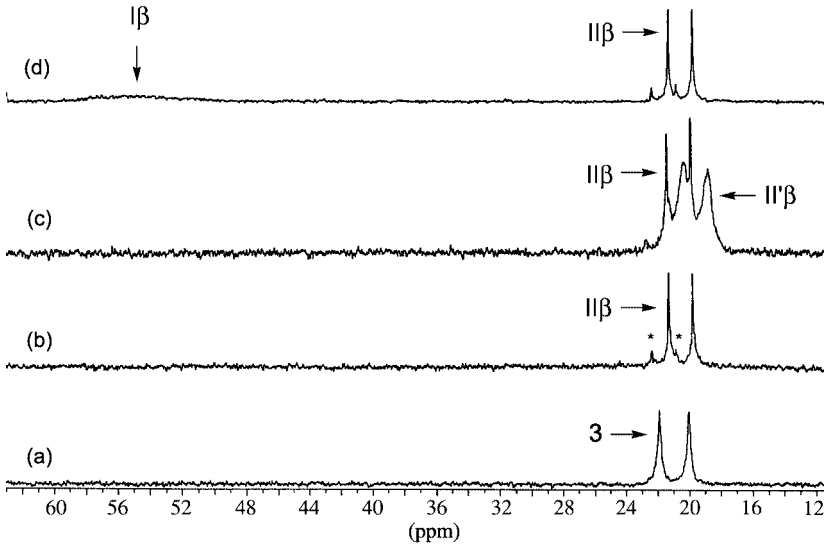

Figure 4. $^{31}P\{^1H\}$ HPNMR spectra under CO pressure of complex **3** in $CDCl_3$ solution. (a) Under N_2, (b) under 20 bar of CO, after 3 min, (c) under 20 bar of CO, after 14 h, (d) after depressurization. The asterisk denotes a small amount of a unidentified rhodium compound.

resonance to a pentacoordinate Rh^I complex resulting from a further rhodium carbonylation of **IIβ** at this high CO pressure, although we have no further spectroscopic evidence to support this assignment at the moment. Depressurization of the NMR tube and purging the solution from dissolved CO with a dinitrogen stream removed the signal due to **II′β** and restored the equilibrium between complexes **Iβ** and **IIβ** [see spectrum (d), Figure 4]. The above IR and NMR observations are summarized in Scheme 4.

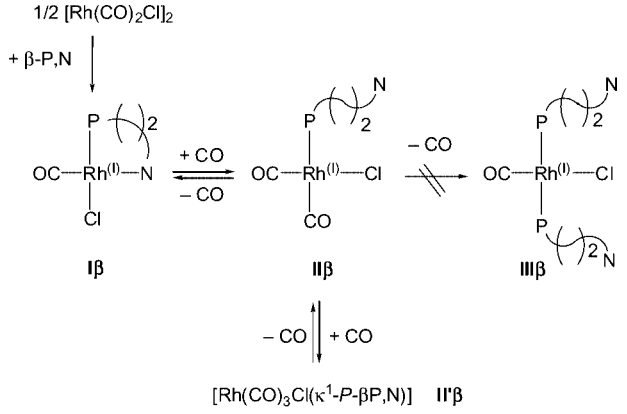

Scheme 4.

Both experiments confirm the occurrence of an equilibrium between **Iβ** and **IIβ** depending on the CO pressure as well as the hemilabile character of the **β-P,N** ligand in Rh^I complexes. The combined IR and HPNMR experiments unambiguously prove the preference for keeping the amino group uncoordinated, under high CO pressure, in both β- and γ-P,N Rh^I complexes, as previously shown for the related α-P,N Rh^I complexes, resulting in a selective κ^1-P coordination mode. We now wish to examine the effects of the dangling amine group on the catalytic properties of the Rh-P,N hydroformylation.

Catalytic Styrene Hydroformylation with Rh-Amino-Phosphane Complexes

The catalytic properties of different systems obtained from either $[RhCl(COD)]_2$ or $[Rh(acac)(CO)_2]$ and a variety of amino-phosphane ligands (see Scheme 5) in styrene hydroformylation tests are shown in Table 2.

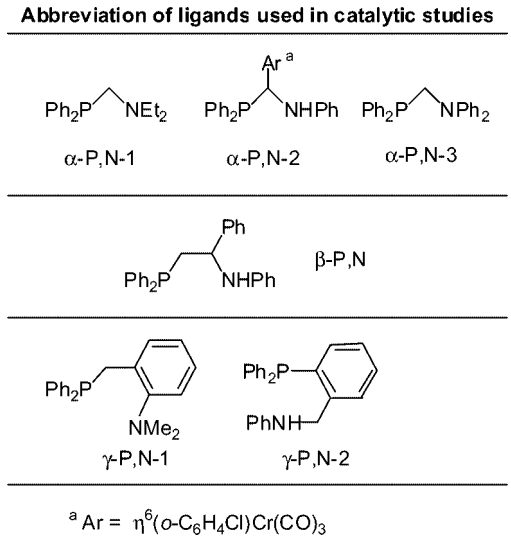

Scheme 5.

All catalytic runs were monitored by periodical withdrawal of aliquots from the autoclave. The conversion was found to be essentially linear with time, without any induction period. Thus, each reported TOF is obtained from a plot obtained by using several data points and is affected by a small error (ca. ±5%, see experimental section for details). All investigated catalysts afforded complete chemoselectivities (no product other than aldehydes are observed) and essentially the same regioselectivity, namely ca. 9:1 in favor of the branched product, which is standard for styrene hydroformylation with rhodium catalysts.[29]

A blank experiment carried out with $[RhCl(COD)]_2$ and PPh_3 (run 1) showed no activity whatsoever under our mild catalytic conditions. As previously reported,[30] the transformation of the chloride precursor to the catalytically active hydride complex requires an external base to trap the HCl equivalent which forms as a by-product during the initial H_2 activation step. The addition of one equivalent of Ph_2NH or NEt_3 as an external base to the previous PPh_3-based catalyst led to a weak catalytic activity (run 2). When an amino group, on the other hand, is incorporated into the tertiary phosphane ligand (runs 3 to 7), a similar or

Table 2. Activity of Rh^I-P,N complexes in styrene hydroformylation catalysis.

Run[a]	Catalytic precursor	Ligand (1 equivalent)	TOF[b] [h^{-1}]	b/l ratio[c]
1	$[RhCl(COD)]_2$	PPh_3	<1	–
2a	$[RhCl(COD)]_2$	PPh_3 + Ph_2NH	4±0.2	88:12
2b	$[RhCl(COD)]_2$	PPh_3 + NEt_3	10±0.5	87:13
3a	$[RhCl(COD)]_2$	$Ph_2P(o\text{-}C_6H_4\text{–}CH_2NHPh)$ (**γ-P,N-2**)	4±0.2	91:9
3b	$[RhCl(COD)]_2$	Ph_2PCH_2 ($o\text{-}C_6H_4\text{–}NMe_2$) (**γ-P,N-1**)	8±0.4	92:8
4	$[RhCl(COD)]_2$	$Ph_2PCH_2CH(Ph)NHPh$ (**β-P,N**)	13±1	91:9
5	$[RhCl(COD)]_2$	$Ph_2PCH_2NPh_2$ (**α-P,N-3**)	15±1	89:11
6	$[RhCl(COD)]_2$	$Ph_2PCH(Ar)NHPh$[d] (**α-P,N-2**)	42±2	89:11
7	$[RhCl(COD)]_2$	$Ph_2PCH_2NEt_2$ (**α-P,N-1**)	230±12	91:9

[a] Conditions: $[RhCl(COD)]_2$ (2.62×10^{-2} mmol) or $[Rh(acac)(CO)_2]$ (5.23×10^{-2} mmol), styrene/Rh = 1000, $CHCl_3$ (35 mL), 55 °C, *p*(syngas) = 600 psi. [b] TOF calculated from the slope of the conversions as a function of time. [c] Regioselectivity determined after complete conversion or from initial conversion rate for the faster catalytic reactions. [d] Ar = $\eta^6(o\text{-}C_6H_4Cl)Cr(CO)_3$.

higher (quite substantial in some cases) increase of catalytic activity resulted. Although the formation of a very active phosphane-free carbonyl species could be envisaged during the ligand scrambling process for the γ-amino-phosphane complexes **IIγ** (see Scheme 3), the lower activities observed with the complexes (runs 3a,b) indicate that either this scrambling process does not take place under the catalytic conditions (high CO pressure) or that the species formed by such a process does not possess a very high catalytic activity. The conversion rate became progressively greater as the number of carbon atoms in the ligand backbone bridging the P and N donor ends decreased from 3 to 1. A jump in activity was particularly evident on going from the γ- (3 carbon atoms) to the α-P,N ligand (1 carbon atom), with essentially identical Brønsted basicities for the dangling amino groups (runs 3a, 4, and 6). The effects of the amine basicity on the catalyst activity were then investigated.

Nitrogen Basicity

A comparison between runs 5 and 7 shows that when the uncoordinated NPh_2 moiety in the α-P,N ligand is replaced by the more basic NEt_2 unit, the activity (TOF) increases dramatically from 15 to 230 h^{-1}. A similar, albeit more moderate, effect is also observed for a similar change in γ-P,N ligands in which the amino group is farther from the metallic center (see run 3a and 3b). These observations highlight the fact that the presence of an uncoordinated basic function in proximity to the metal center has a beneficial effect on the overall catalytic activity. A similar activity/basicity relationship for an uncoordinated amine function was pointed out by Reetz et al.,[12] who reported that the activity of rhodium cationic complexes in styrene or octene hydroformylation increased significantly when the dppp ligand [dppp = $Ph_2P(CH_2)_3PPh_2$] was replaced by an amino-diphosphane ligand [$Ph_2PCH_2N(Ph)CH_2PPh_2$], in which the nitrogen atom remains uncoordinated. It is to be noted that this conclusion is exactly opposite to that of Abu-Gnim and Amer, although both the ligands and conditions employed by them are apparently quite similar to ours.[11] It is possible that such a divergence comes from Amer's conclusion, which is based on the TON values. Such data are obviously less significant than the related TOF and, in addition, have been calculated from only one catalytic experiment per ligand used, with different reaction times as a function of the ligand.[11] Our straightforward interpretation of the activity results presented in Table 3 is based on the fact that all P,N ligands display an uncoordinated amine function under catalytic conditions, as demonstrated above. Additionally, the presence of the free internal base is not devoid of consequence for the catalytic efficiency because the whole system becomes more efficient as the P–N distance decreases, respectively going from γ-, β- to α-P,N ligands, and as its basicity increases.

Rhodium Acetylacetonate Catalyst

Under the assumption that the HCl molecule originating from the chloride catalyst precursor and H_2 is scavenged by the dangling amine function, the latter would be converted into an ammonium function. Thus, the active catalyst would turn over in the ammonium form, rather than in the free amine form. In order to check the effect of this protonation process on the catalytic activity, experiments have also been carried out using [Rh(acac)$(CO)_2$] as the catalytic precursor. This allows the uncoordinated amine to remain in the neutral form during the catalytic cycle, since the active hydride species forms with elimination of acetylacetone rather than HCl. These experiments were only carried out with the α-P,N ligands, and the results are collected in Table 3. Generally, [Rh(acac)$(CO)_2$] is known to be a better catalytic precursor than [RhCl(COD)]$_2$ and, indeed, a comparison between runs 1 (Table 2) and 8 (Table 3) shows that this is true also in our case.

The activity in the presence of PPh_3 (see run 8, Table 3) remains nevertheless lower than in the presence of the α-P,N ligands (see runs 9, 10, and 11, Table 3), highlighting the beneficial effect of the free amine on the catalysis rate-determining step. We then ran an additional catalytic experiment which consisted of the addition of one equivalent of NEt_3 into the **α-P,N-3** rhodium chloride catalytic system. This led to better conversions (TOF = 220 h^{-1}, run 12) than the NEt_3-free system (TOF = 15 h^{-1}, run 5), and rather close to those obtained with the Rh-acetylacetonate catalytic precursor (TOF = 285 h^{-1}, run 10).

Discussion

The new results reported in this contribution show that all P,N ligands are κ^1-P coordinated to Rh^I under hydroformylation conditions, no matter the distance between the N and P atoms, and that the catalytic activity is enhanced by the proximity of the amine function and by its basicity. The role of the free amine group can be proposed at two different levels. First, we recall that no induction time is ob-

Table 3. Activity of α-P,N-based Rh^I complexes in styrene hydroformylation catalysis.

Run[a]	Catalytic precursor	Ligand (1 equivalent)	TOF[b] [h^{-1}]	b/l ratio
8	Rh(acac)$(CO)_2$	PPh_3	130 ± 7	93:7
9	Rh(acac)$(CO)_2$	$Ph_2PCH(Ar)NHPh$[b]	170 ± 9	88:12
10	Rh(acac)$(CO)_2$	$Ph_2PCH_2NPh_2$	285 ± 13	90:10
11	Rh(acac)$(CO)_2$	$Ph_2PCH_2NEt_2$	325 ± 16	92:8
12	[RhCl(COD)]$_2$	$Ph_2PCH_2NPh_2$ + NEt_3[c]	220 ± 11	90:10

[a] Conditions described in Table 2. [b] Ar = η^6(*o*-C_6H_4Cl)$Cr(CO)_3$. [c] 1 Equivalent relative to the rhodium complex.

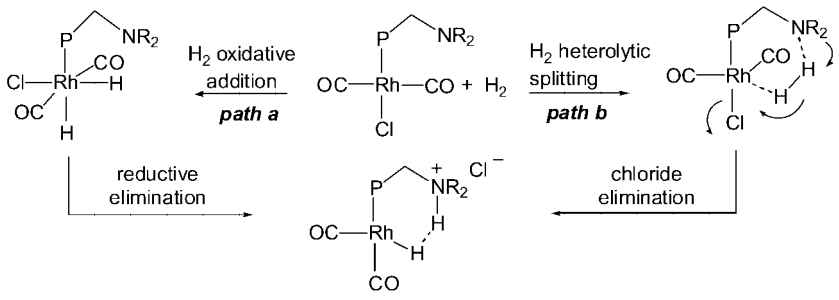

Scheme 6.

served for the generation of the catalytically active species. In order to generate the active Rh–H species, rhodium(I) chloride precursors typically show induction periods in the catalytic process because of the need to eliminate HCl after the dihydrogen oxidative addition to rhodium. The addition of an external amine favors this process and reduces or even eliminates the induction time.[30] In our own hands, $[RhCl(COD)]_2$ still affords a very active catalyst in the absence of any added phosphane ligand under the same conditions given in Table 3, but only after quite a long induction period (>3 h). It seems therefore reasonable to us that the dangling nitrogen function plays an important role in assisting the rapid formation of the Rh–H active species. We see two possible ways by which this "assistance" effect can operate. A first possibility involves, after the initial H_2 oxidative addition, the N-assisted promotion of HCl elimination from the intermediate Rh^{III} dihydride (see Scheme 6, path a). On the other hand, an alternative mechanistic pathway could involve heterolytic cleavage of H_2 (see Scheme 6, path b). Indeed, many authors have proposed a base-assisted H_2 heterolytic splitting in relation to other catalytic processes (i.e. involving Ru,[31–34] Ir,[35] Pd,[36] and Rh[37]) over the last few years. Heterolytic splitting of H_2 is also shown by computational methods to be kinetically and thermodynamically more favorable than the classical dihydrogen oxidative addition for the interaction with the rhodium complex $Rh(PH_3)_2(HCO_2)$ in the presence of NH_3.[38] Consequently, a similar H_2 heterolytic activation process seems a reasonable possibility also for the rhodium hydroformylation catalytic systems here described, in particular with the basic $Ph_2PCH_2NEt_2$ ligand (see Scheme 6). In either case, the HCl produced during the activation step is likely to be trapped by the nearby amine function. However, this activation step cannot be enhancing the activity, because the chloride precursor is not the resting state of the catalytic cycle.

The second level where the external base is likely to have an effect concerns the rate-determining step of the catalytic cycle (*rds*), namely the hydrogenolysis of the rhodium acyl intermediate. Detailed kinetic and mechanistic studies carried out by van Leeuwen et al. have shown that the rate-determining step in rhodium catalyzed hydroformylation may be either the olefin insertion into the Rh–H bond or the Rh-acyl hydrogenolysis, depending on the ligand nature and on the conditions.[29,39] In the cases at hand, we have collected preliminary evidence, via H/D isotopic exchange experiments, that the hydrogenolysis is rate determining. Details of these studies are provided in a separate paper[40] In addition, no evidence for the accumulation of a hydride intermediate (as required if the olefin insertion step were rate determining) was obtained by HPNMR (vide infra).

We must now attempt to rationalize two different observations: (*i*) a proximal *free* amine function has a beneficial effect (i.e. see the experiments carried out with the acetylacetonate catalyst or with the chloride in the presence of an external base, cf. runs 12 and 2b); (*ii*) the beneficial effect is observed even when the dangling amine function is likely turned into an ammonium derivative (i.e. see all the experiments carried out with the chloride catalyst, without the use of an external base, runs 3–7).

Concerning the first point, we assume that the action of the uncoordinated amine function on the *rds* is similar to that proposed above for the activation of the chloride precursor, see Scheme 7. The greater activity could in principle be interpreted on the basis of two possible mechanistic routes. The first one (path a, Scheme 7) involves H_2 oxidative addition followed by aldehyde reductive elimination. On the basis of this mechanism, we would argue that the free amine ligand somehow helps either one or both of these elementary steps. However, the lack of interaction between the rhodium-acyl species and the dangling nitrogen moiety does not allow an obvious rationalization of the observed

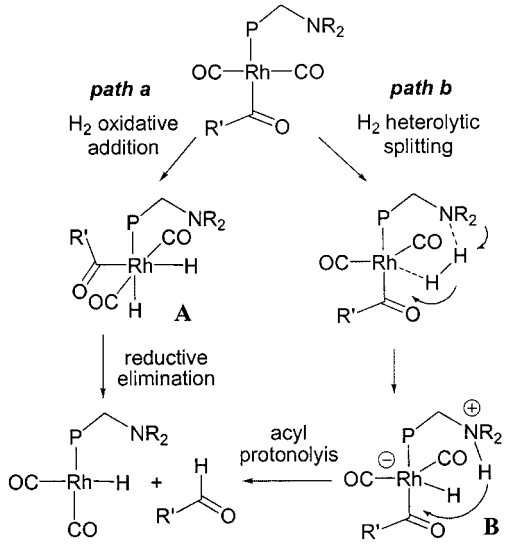

Scheme 7.

effect. The second pathway (path b, Scheme 7) involves a base-assisted heterolytic H_2 splitting, leading to a zwitterionic rhodium monohydride intermediate. The latter would be stabilized by a P,N-ligand bearing a uncoordinated ammonium end. According to this mechanism, increasing the amine basicity could lower the activation barrier leading to the zwitterionic intermediate, thereby accelerating the *rds*. The aldehyde would then be formed by protonolysis of the rhodium-acyl bond by the dangling ammonium group, rather than by a reductive elimination process.

Clearly, the accelerating effect just discussed cannot be provided when the amine function is protonated. However, it is possible to envisage a proton exchange process, whereby the ammonium hydride derivative **B** formed during the catalyst activation step may equilibrate with the amine–chloride precursor **A** to yield an inactive ammonium chloride species **D** and an active amine–hydride complex **C**, identical to that obtained from the acetylacetonate precursor (see Scheme 8). Consequently, the different accelerating effect that is observed for the chloride systems in the absence of external base (runs 3–7) may be attributed to the presence of the equilibrium species **D**, which would again operate through the same mechanism of Scheme 7, the extent of the effect being a function of the equilibrium amount of that species. Acyl complexes are known to give hydrogenolysis even without the assistance of an internal amine function. However, the presence of an internal base increases the activity of the rhodium catalyst, to a growing extent as its basicity increases (see runs 8 through 11) and could then promote the hydrogenolysis step through a mechanism encompassing the H_2 heterolytic splitting.

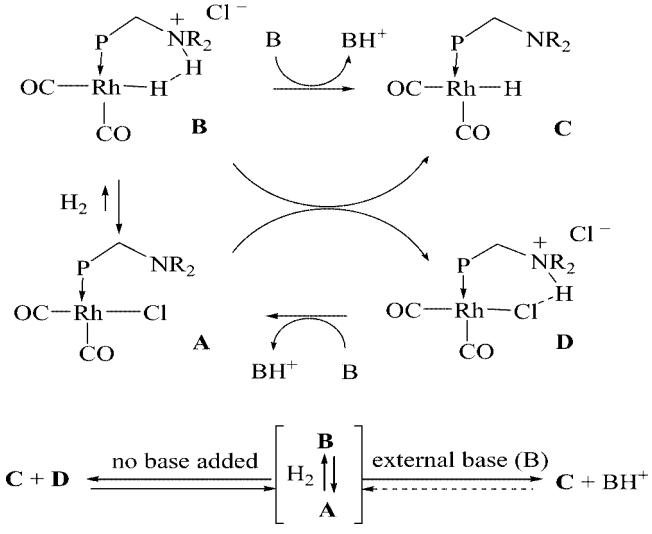

Scheme 8.

In order to obtain further mechanistic information, we have carried out a ^1H HPNMR study of the $[RhCl(COD)]_2$-$Ph_2PCH_2NPh_2$ mixture in $CDCl_3$ under syngas (20 atm), approaching the experimental conditions of the catalytic runs. No Rh–H species could be observed under these conditions. This observation suggests that the **A**/**B** equilibrium proposed in Scheme 8 is only weakly shifted to the Rh–H hydride species **B**. The most active species **C** would then form only in minor proportion, leading to a low catalytic activity. According to Scheme 8, the amount of **C** could be increased only upon addition of a strong external base. On the other hand, the catalytic formation of aldehyde was immediately observed after the styrene introduction into the HPNMR tube, although the hydride resonance remained undetected. The latter result is consistent with the proposition that the olefin insertion step is not the *rds* for this system.

Conclusions

The IR and ^{31}P HPNMR studies reported in this contribution have shown that the coordination properties of a variety of amino-phosphane ligands in Rh^I complexes depend on the length of the P,N backbone. The γ-P,N ligands behave as κ¹-*P*-α-amino-phosphanes, whereas the β-P,N amino-phosphane leads to a solution equilibrium between κ²-*P,N* and κ¹-*P*-coordination modes, depending on the CO pressure. Under hydroformylation conditions, however, all the investigated Rh-amino-phosphane precatalysts exist as monodentate $[RhCl(CO)_2(\kappa^1\text{-}P\text{-}P,N)]$ complexes with a noncoordinated nitrogen function. The reported catalytic runs demonstrate that the dangling amino group favors the formation of the Rh–H active species when using $[RhCl(COD)]_2$ as the catalytic precursor and that both the basicity of the nitrogen end and its distance from the metal center have a crucial effect on the turnover frequency. The hydride formation could occur either by H_2 heterolytic splitting (assisted by the nearby amino group) or by a classical oxidative addition (with the amino group assisting the subsequent HCl reductive-elimination). Theoretical calculations are currently in progress in order to elucidate the preferred mechanistic pathway. We also suggest that the dangling amino group could take an additional mechanistic function as promoter of the hydrogenolysis step through a second heterolytic H_2 splitting. Isotopic H/D exchange studies under catalytic conditions using chiral P,N ligands, which are reported in a separate contribution,[40] provide additional mechanistic details in hydroformylation catalysis via rhodium amino-phosphane systems.

Experimental Section

All manipulations were carried out under purified argon using standard Schlenk techniques. All solvents were dried and deoxygenated prior to use by standard methods. Standard pressure NMR measurements [^1H, $^{13}C\{^1H\}$, and $^{31}P\{^1H\}$] were carried out with a Bruker DRX300 spectrometer in $CDCl_3$ at room temperature. The peak positions are reported with positive shifts in ppm downfield of TMS as calculated from the residual solvent peaks [^1H and $^{13}C\{^1H\}$] or downfield of external 85% H_3PO_4 (^{31}P). The high-pressure NMR (HPNMR) spectra were recorded by using a standard 10-mm probe tuned to ^{31}P and ^1H nuclei on a BRUKER AC 200 spectrometer operating at 81 MHz. The HPNMR experiments were performed in a 10-mm sapphire tube (Saphikon Inc., NH) charged with a solution of precatalyst (10 mg of P,N ligand, plus

0.5 equiv. of Rh precursor) in $CDCl_3$ (2 mL) under nitrogen, after which the first spectrum (reference) was recorded at room temp. The tube was then pressurized with CO 20 atm at room temp. The variable temperature experiment was started on a Bruker AC 200 spectrometer, recording a sequence of spectra up to 80 °C. After a chosen time, the probe was cooled to room temperature and another spectrum was recorded. The last spectrum was taken after venting the tube and flushing with nitrogen. The coordinated 1,5-COD (1,5-cyclooctadiene) C and H nuclei are labeled from 1 to 8, C^1 and C^2 being *trans* to P.

CAUTION: *All manipulations involving high pressure are potentially hazardous. Safety precautions must be taken at all stages of NMR studies involving high pressure tubes.*

All IR spectra were recorded in CH_2Cl_2 solution with a Bruker IFS 66 V spectrophotometer with KBr optics and the absorption vibration bands are given in cm^{-1}. Elemental analyses were carried out by the analytical service of the L.S.E.O. with a Fisons Instruments EA1108 analyzer. The commercial compounds PPh_3, Ph_2NH, $[RhCl(COD)]_2$, $[Rh(acac)(CO)_2]$, and $[Rh(CO)_2Cl]_2$ were used as received. The ligands $Ph_2PCH_2NEt_2$, $Ph_2PCH_2NPh_2$, $Ph_2PCH(Ar)NHPh$ {Ar = *o*-C_6H_4Cl or *o*-$C_6H_4Cl[Cr(CO)_3]$}, $Ph_2PCH_2CH(Ph)NHPh$, Ph_2PCH_2(*o*-C_6H_4–NMe_2) (γ-P,N-1), and Ph_2P(*o*-C_6H_4–CH_2NHPh) (γ-P,N-2) were prepared according to literature.[13,14,17,41–44] The synthesis of complex [RhCl(COD)(α-P,N)] **1** with α-P,N=Ph_2PCH(*o*-$C_6H_4Cl[Cr(CO)_3]$)NHPh has previously been described.[18]

Synthesis of [RhCl(COD)(P,N)] Complexes

The syntheses of the [RhCl(COD)(P,N)] complexes were generally carried out as follows. A mixture of $[RhCl(COD)]_2$ and P,N ligand were dissolved in CH_2Cl_2 (5 mL). The yellow solution obtained was stirred for 1 h. Addition of pentane afforded yellow or orange microcrystals which were isolated and dried in vacuo.

[RhCl(COD)(γ-P,N-1)] (2): $[RhCl(COD)]_2$ (84.4 mg, 0.171 mmol), **γ-P,N-1** (109 mg, 0.341 mmol) gave 144 mg of **2**, yield 75%. ^1H NMR: δ = 8.81–7.12 (m, 14 H, arom.), 5.61 (s, 2 H, C_8H_{12}, olefinic protons, *trans* to P), 4.21 [d, $^2J_{(P,H)}$ = 11.6 Hz, 2 H, PCH_2], 2.93 (s, 2 H, C_8H_{12}, olefinic protons, *cis* to P), 2.48 (s, 3 H, NCH_3), 2.49–1.86 (m, 8 H, C_8H_{12}, aliph. H) ppm. $^{31}P\{^1H\}$ NMR: δ = 30.1 [d, $^1J_{(Rh,P)}$ = 150 Hz] ppm. $^{13}C\{^1H\}$ NMR: δ = 154.1–120.2 (m, 18 C, arom.), 104.3 (m, 2 C, $C^{1,2}$), 70.9 (s, 1 C, C^5), 70.7 (s, 1 C, C^6), 45.3 (s, 2 C, NCH_3), 33.3 (s, 2 C, $C^{3,8}$), 29.3 (s, 2 C, $C^{4,7}$), 28.5 [d, $^2J_{(P,C)}$ = 21 Hz, 1 C, PCH_2] ppm. $C_{29}H_{34}ClNPRh$ (565.92): calcd. C 61.55, H 6.05, N 2.48; found C 61.09, H 5.66, N 3.09.

[RhCl(COD)(β-P,N)] (3): $[RhCl(COD)]_2$ (85 mg, 0.172 mmol) and **β-P,N** (131 mg, 0.344 mmol) gave 152 mg of **3**, yield 80%. ^1H NMR: δ = 8.09–6.72 (m, 20 H, arom.), 7.02 [d, $^3J_{(P,H)}$ = 7 Hz, 1 H, NH, exchange with D_2O], 4.78 (m, 1 H, NCH^c), 3.36 [dt, $^2J_{(P,H^a)}$ = $^3J_{(H^a,H^b)}$ = 14, $^3J_{(H^a,H^c)}$ = 4 Hz, 1 H, PCH^a], 2.64 [t, $^2J_{(P,H^b)}$ = $^3J_{(H^b,H^a)}$ = 14 Hz, 1 H, PCH^b], 2.38–1.75 (m, 6 instead of 8 H, C_8H_{12}, aliph. H) ppm. The olefinic protons were not observed at room temp. due to an olefin rotation dynamic process. $^{31}P\{^1H\}$ NMR: δ = 21.7 [d, $^1J_{(Rh,P)}$ = 150 Hz] ppm. $^{13}C\{^1H\}$ NMR: δ = 147.1–114.9 (m, 24 C, arom.), 105.0 (s, very br., 2 C, $C^{1,2}$ of COD), 71.0 (s, very br., 2 C, $C^{5,6}$ of COD), 57.1 (s, 1 C, NCH), 37.7 [d, $J_{(P,C)}$ = 22 Hz, 1 C, PCH], 31.3 (br. s, 4 C, $C^{3,4,7,8}$ of COD) ppm. IR: $\tilde{\nu}$ = 3324 (m, ν_{NH}) cm^{-1}. $C_{34}H_{36}ClNPRh{\cdot}0.5CH_2Cl_2$ (670.45): calcd. C 61.75, H 5.52, N 2.09; found C 62.15, H 5.77, N 2.23.

[RhCl(CO)(β-P,N)] (Iβ): $[RhCl(CO)_2]_2$ (36.1 mg, 0.093 mmol) and **β-P,N** (71 mg, 0.186 mmol) gave 76 mg of **Iβ**, 57% yield. ^1H NMR: δ = 8.22–6.83 (m, 20 H, arom.), 6.84 [d, $^3J_{(P,H)}$ = 10.8 Hz, 1 H, NH, exchange with D_2O], 3.91 (m, 1 H, NCH^c), 3.58 [dt, $^2J_{(P,H^a)}$ = $^3J_{(H^a,H^b)}$ = 14, $^3J_{(H^a,H^c)}$ = 4 Hz, 1 H, PCH^a], 2.86 [dt, $^2J_{(P,H^b)}$ = $^3J_{(H^b,H^a)}$ = 14, $^3J_{(H^b,H^c)}$ = 2 Hz, 1 H, PCH^b] ppm. $^{31}P\{^1H\}$ NMR: δ = 56.4 [d, $^1J_{(Rh,P)}$ = 168 Hz] ppm. $^{13}C\{^1H\}$ NMR: δ = 188.5 [dd, $^1J_{(Rh,C)}$ = 74, $^2J_{(P,C)}$ = 18 Hz according to CO *cis* to P,[45] 1 C, C=O], 145.7–125.5 (m, 24 C, arom.), 8.51 [d, $^2J_{(P,C)}$ = 8.6 Hz, 1 C, NCH], 38.8 [d, $J_{(P,C)}$ = 26 Hz, 1 C, PCH] ppm. IR: $\tilde{\nu}$ = 1986 cm^{-1} (vs, ν_{CO}) and ν_{NH} not observed. $C_{27}H_{24}ClNOPRh{\cdot}0.5CH_2Cl_2$ (590.28): calcd. C 55.90, H 4.24, N 2.37; found C 55.64, H 4.38, N 2.54.

***trans*-[RhCl(CO)(γ-P,N-1)$_2$] (IIIγ):** $[RhCl(CO)_2]_2$ (39 mg, 0.098 mmol) and **γ-P,N-1** (125 mg, 0.392 mmol) gave 113 mg of **IIIγ**, yield 71%. ^1H NMR: δ = 8.39–6.93 (m, 28 H, arom.), 4.40 (t not resolved, 4 H, PCH_2), 2.30 (s, 6 H, NCH_3). $^{31}P\{^1H\}$ NMR: δ = 31.20 [d, $^1J_{(Rh,P)}$ = 126 Hz] ppm. $^{13}C\{^1H\}$ NMR: δ = 188.0 [dt, $^1J_{(Rh,C)}$ = 76, $^2J_{(P,C)}$ = 14 Hz according to CO *cis* to both P,[45] 1 C, C=O], 154.2–120.1 (m, 36 C, arom.), 45.2 (s, 4 C, NCH_3). 26.8 [t, $J_{(P,C)}$ = 27 Hz, 2 C, PCH_2] ppm. IR: $\tilde{\nu}$ = 1974 (vs, ν_{CO}) cm^{-1}. $C_{43}H_{44}ClN_2OP_2Rh$ (805.13): calcd. C 64.15, H 5.51, N 3.48; found C 64.46, H 5.55, N 3.34.

Formation of the Unstable *cis*-[RhCl(CO)$_2$(γ-P,N-1)] (Iiγ). Method A: A mixture of $[RhCl(CO)_2]_2$ (19.5 mg, 0.050 mmol) and **γ-P,N-1** (32 mg, 0.098 mmol) was dissolved in $CDCl_3$ (0.7 mL). After 10 min, the mixture was analyzed by ^1H and $^{31}P\{^1H\}$ spectroscopy showing **IIγ** as the major complex. ^1H NMR: δ = 7.75–7.03 (m, 14 H, arom.), 4.27 [d, $^2J_{(P,H)}$ = 12 Hz, 2 H, PCH_2], 2.34 (s, 6 H, NCH_3) ppm. $^{31}P\{^1H\}$ NMR: δ = 31.1 [14%, d, $^1J_{(Rh,P)}$ = 125 Hz] ppm for **IIIγ** and 27.4 [86%, d, $^1J_{(Rh,P)}$ = 126 Hz] ppm for **IIγ**. After ca. 0.75 h and 12 h, the $^{31}P\{^1H\}$ NMR gave 1:4.5 and 1:2 ratios respectively for the **IIIγ/IIγ** mixture complexes. The above procedure was repeated in CH_2Cl_2 instead of chloroform. The atmosphere was then purged with CO and monitored by infrared. After 2 min, the pure dicarbonyl was formed. No ^{13}C NMR spectrum was recorded due to the increase of the ratio **IIIγ/IIγ** with time. The above procedure was repeated in CH_2Cl_2 and a slow diffusion of pentane to the yellow solution afforded poor quality yellow crystals which were identified as the complex **IIIγ**.

Method B: CO was introduced into a solution of [RhCl(COD)(**γ-P,N-1**)], **1a** (35 mg, 0.061 mmol) in CH_2Cl_2 (4 mL). Under CO and after 2 min, the IR spectrum showed only the pure dicarbonyl complex **IIγ** at 2092 and 2010 cm^{-1} (both vs, ν_{CO}), and this had not changed after two days under CO.

Formation of the Unstable *cis*-[RhCl(CO)$_2$(β-P,N)] (Iiβ). Method A: CO was introduced into a solution of [RhCl(COD)(β-P,N)] **1b** (42 mg, 0.071 mmol) in CH_2Cl_2 (4 mL). An IR spectrum was recorded after 2 min and showed a mixture of monocarbonyl complex **Iβ** at 1986 cm^{-1} and dicarbonyl complex [RhCl(CO)$_2$(κ-*P*-P,N)] **IIβ** at 2011 and 2092 cm^{-1}. The ratio between the two complexes did not change after two days under CO.

Method B: A mixture of $[RhCl(CO)_2]_2$ (25.6 mg, 0.066 mmol) and β-P,N (54 mg, 0.131 mmol) was dissolved in $CDCl_3$ (1 mL). After 10 min, CO was introduced into the solution and the mixture was analyzed by ^1H and $^{31}P\{^1H\}$ NMR spectroscopy. The NMR spectra show a mixture of **IIβ** and **Iβ** in 1:2.5 ratio. ^1H NMR of **IIβ**: δ = 8.12–5.63 (m, 28 H, arom.), 5.78 [d, $^3J_{(P,H)}$ = 6 Hz, 2 H, NH, exchange with D_2O], 4.14 (m, 2 H, NCH), 3.58 (m, 2 H, PCH^a), 2.45 (m, 2 H, PCH^b) ppm. $^{31}P\{^1H\}$ NMR of **IIβ**: δ = 21.11 [d, $^1J_{(Rh,P)}$ = 122 Hz] ppm. No $^{13}C\{^1H\}$ NMR spectrum was recorded due to the low solubility of **IIβ** in $CDCl_3$ and $(CD_3)_2CO$.

Crystal Structure Determination of Complex IIIγ: Intensity data were collected with a Nonius Kappa CCD at 230 K. The structure was solved by the heavy atom method and refined by full-matrix

least-squares methods[46] with the aid of the WINGX program.[47] Non-hydrogen atoms were anisotropically refined. Hydrogen atoms were included in calculated positions and refined with a riding model. Crystallographic data for compound **IIIγ** are reported in Table 4.

Table 4. Crystal data and structure refinement for **IIIγ**.

Compound	**IIIγ**
Formula	$C_{43}H_{44}ClN_2OP_2Rh$
M	805.1
T [K]	230(2)
Crystal system	monoclinic
Space group	$C2/c$
a [Å]	13.9791(4)
b [Å]	17.7355(8)
c [Å]	17.4564(8)
β [°]	110.320(2)
V [Å^3]	4058.6(3)
Z	4
$F(000)$	1664
D_{calc} [g/cm^3]	1.318
Diffractometer	Enraf–Nonius KappaCCD
Scan type	mixture of φ rotations and ω scans
λ [Å]	0.71073
μ [mm^{-1}]	0.599
Crystal size [mm^3]	0.6×0.5×0.5
$\sin(\theta)/\lambda$ max. [Å^{-1}]	0.65
Index ranges	h: –17; 18
	k: –22; 22
	l: –18; 22
Absorption correction	SCALEPACK
RC = reflections collected	11009
IRC = independent RC	4587 [R(int) = 0.05]
IRCGT = IRC and [$I > 2\sigma(I)$]	3262
Refinement method	full-matrix least squares on F^2
Data / restraints / parameters	4587 / 0 / 228
R for IRCGT	R_1[a] = 0.0444, wR_2[b] = 0.0934
R for IRC	R_1[a] = 0.0779, wR_2[b] = 0.1044
Goodness-of-fit[c]	1.021
Largest diff. peak and hole [e·Å^{-3}]	0.47 and –1.02

[a] $R_1 = \Sigma(||F_o| - |F_c||)/\Sigma|F_o|$. [b] $wR_2 = \{\Sigma w(F_o^2 - F_c^2)^2/\Sigma[w(F_o^2)^2]^{1/2}\}$ where $w = 1/[\sigma^2(F_o^2) + (0.053P)^2]$, $P = [\max(F_o^2,0) + 2\times F_c^2]/3$. [c] Goodness of fit = $[\Sigma w(F_o^2 - F_c^2)^2/(N_o - N_v)]^{1/2}$.

CCDC-250351 contains the supplementary crystallographic data for this paper. These data can be obtained free of charge from The Cambridge Crystallographic Data Centre via www.ccdc.cam.ac.uk/data_request/cif.

Catalytic Runs: The hydroformylation reactions were carried out in a 300-mL stainless-steel Parr autoclave equipped with a magnetic drive, an internal glass vessel, and an immersion tube connected to a valve for solution withdrawals under pressure. The temperature was controlled by a rigid heating mantle and a single loop cooling coil. The autoclave was purged three times under vacuum/argon before introducing the catalytic solution. The 1:1 CO/H_2 mixture was prepared by mixing the pure gases in a 500-mL stainless-steel cylinder before introduction into the autoclave at the desired pressure (see Table 1 and Table 2). The zero time for kinetic runs was considered as the time at which the desired pressure was reached inside the autoclave. In order to maintain temperature and pressure conditions as constant as possible during each kinetic run, only a few mL of catalytic solution mixture were carefully withdrawn each time from the autoclave. The $CHCl_3$ or THF solvent was then rotary evaporated at room temperature and the yellow-orange residue was analyzed by ^1H and $^{13}C\{^1H\}$ NMR spectroscopy. The experimental error on the TOF determination was carried out from the TOF values obtained from three successive runs using three times the same solution for two different catalytic systems (run, 5 and 10). The experimental error for other catalytic runs has been estimated on the basis of the determination as above.

Acknowledgments

This work was supported by COST D29 (WG009/03) and by the EC through the contracts HPRN-CT-2002–00176 (HYDROCHEM) and MRTN-CT-2003–503864 (AQUACHEM) and the contribution is kindly acknowledged. We are also grateful to the Ministère de la Recherche, the Centre National de la Recherche Scientifique (CNRS) and the Conseil Régional de Bourgogne for support of this work. J.-M. C. thanks the Ministère de la Recherche for a Ph. D. fellowship. HPNMR measurements have been possible through the NMR service of "FIRENZE HYDROLAB": a project sponsored by a generous grant by Ente Cassa di Risparmio di Firenze.

[1] E. Drent, P. Arnoldy, P. H. M. Budzelaar, *J. Organomet. Chem.* **1993**, *455*, 247–253.
[2] K. N. Gravilov, A. I. Polosukhin, *Russ. Chem. Rev.* **2000**, *69*, 661–682.
[3] P. Denis, A. Jean, J. F. Crizy, A. Mortreux, F. Petit, *J. Am. Chem. Soc.* **1990**, *112*, 1292–1294.
[4] H. Yang, M. Alvarez, N. Lugan, R. Mathieu, *J. Chem. Soc. Chem. Commun.* **1995**, 1721–1722.
[5] J.-X. Gao, T. Ikariya, R. Noyori, *Organometallics* **1996**, *15*, 1087–1089.
[6] C. Standfest-Hauser, C. Slugovc, K. Mereiter, R. Schmid, K. Kirchner, L. Xiao, W. Weissensteiner, *J. Chem. Soc., Dalton Trans.* **2001**, 2989–2995.
[7] T. B. Rauchfuss, J. L. Clements, S. F. Agnew, D. M. Roundhill, *Inorg. Chem.* **1977**, *16*, 775–778.
[8] D. M. Roundhill, R. A. Bechtold, S. G. N. Roundhill, *Inorg. Chem.* **1980**, *19*, 284–289.
[9] J. P. Collman, *Acc. Chem. Res.* **1968**, *1*, 136–143.
[10] F. Fache, E. Schultz, M. L. Tommasino, M. Lemaire, *Chem. Rev.* **2000**, *100*, 2159–2231.
[11] C. Abu-Gnim, I. Amer, *J. Mol. Catal.* **1993**, *85*, L275–L278.
[12] M. T. Reetz, S. R. Waldvogel, R. Goddard, *Tetrahedron Lett.* **1997**, *38*, 5967–5970.
[13] J. Andrieu, C. Baldoli, S. Maiorana, R. Poli, P. Richard, *Eur. J. Org. Chem.* **1999**, 3095–3097.
[14] J. Andrieu, J.-M. Camus, J. Dietz, P. Richard, R. Poli, *Inorg. Chem.* **2001**, *40*, 1597–1605.
[15] J. Andrieu, P. Richard, J.-M. Camus, R. Poli, *Inorg. Chem.* **2002**, *41*, 3876–3885.
[16] J. M. Camus, J. Andrieu, P. Richard, R. Poli, *Eur. J. Inorg. Chem.* **2004**, 1081–1091.
[17] J. Andrieu, J. Dietz, R. Poli, P. Richard, *New J. Chem.* **1999**, *23*, 581–583.
[18] J. M. Camus, J. Andrieu, P. Richard, R. Poli, C. Baldoli, S. Maiorana, *Inorg. Chem.* **2003**, *42*, 2384–2390.
[19] X. Liu, A. H. Eisenberg, C. L. Stern, C. A. Mirkin, *Inorg. Chem.* **2001**, *40*, 2940–2941.
[20] L. Dahlenburg, R. Götz, *J. Organomet. Chem.* **2001**, *619*, 88–98.
[21] M. Valentini, K. Selvakumar, M. Wörle, P. S. Pregosin, *J. Organomet. Chem.* **1999**, *587*, 244–251.
[22] A. Aghmiz, A. M. Masdeu-Bulto, C. Claver, D. Sinou, *J. Mol. Catal. A: Chem.* **2002**, *184*, 111–119.
[23] C. Saluzzo, J. Breuzard, S. Pellet-Rostaing, M. Vallet, F. Le Guyader, M. Lemaire, *J. Organomet. Chem.* **2002**, *643*, 98–104.
[24] M. L. Clarke, G. L. Holliday, A. M. Z. Slawin, J. D. Woollins, *J. Chem. Soc., Dalton Trans.* **2002**, 1093–1103.

[25] J. Andrieu, B. R. Steele, C. G. Screttas, C. J. Cardin, J. Fornies, *Organometallics* **1998**, *17*, 839–845.
[26] P. Crochet, J. Gimeno, S. Garcia-Granda, J. Borge, *Organometallics* **2001**, *20*, 4369–4377.
[27] G. A. Luinstra, P. H. P. Brinkmann, *Organometallics* **1998**, *17*, 5160–5165.
[28] I. Yamada, M. Ohkouchi, M. Yamaguchi, T. Yamagishi, *J. Chem. Soc., Perkin Trans. 1* **1997**, 1869–1873.
[29] P. W. N. M. Van Leeuwen, C. Claver (Eds.), *Rhodium Catalyzed Hydroformylation*, Kluwer, Dordrecht, **2000**, vol. 22.
[30] D. Evans, J. A. Osborn, G. Wilkinson, *J. Chem. Soc. (A)* **1968**, 3133–3142.
[31] H. S. Chu, C. P. Lau, K. Y. Wong, W. T. Wong, *Organometallics* **1998**, *17*, 2768–2777.
[32] T. Ohkuma, D. Ishii, H. Takeno, R. Noyori, *J. Am. Chem. Soc.* **2000**, *122*, 6510–6511.
[33] K. Abdur-Rashid, M. Faatz, A. J. Lough, R. H. Morris, *J. Am. Chem. Soc.* **2001**, *123*, 7473–7474.
[34] L. Dahlenburg, R. Götz, *Eur. J. Inorg. Chem.* **2004**, *4*, 888–905.
[35] A. J. Lough, S. Park, R. Ramachandran, R. H. Morris, *J. Am. Chem. Soc.* **1994**, *116*, 8356–8357.
[36] P. Pelagatti, A. Bacchi, M. Carcelli, M. Costa, A. Fochi, P. Ghidini, E. Leporati, M. Masi, C. Pelizzi, G. Pelizzi, *J. Organomet. Chem.* **1999**, *583*, 94–105.
[37] D. Sellmann, G. H. Rackelmann, F. W. Heinemann, *Chem. Eur. J.* **1997**, *3*, 2071–2080.
[38] F. Hutschka, A. Dedieu, *J. Chem. Soc., Dalton Trans.* **1997**, 1899–1902.
[39] S. C. van der Slot, P. C. J. Kamer, P. van Leeuwen, J. A. Iggo, B. T. Heaton, *Organometallics* **2001**, *20*, 430–441.
[40] J. Andrieu, J. M. Camus, C. Balan, R. Poli, *Eur. J. Inorg. Chem.* **2006**, 62–68; following article.
[41] K. Isslieb, R. Kümmel, H. Oehme, I. Meisser, *Chem. Ber.* **1968**, *101*, 3612–3618.
[42] A. L. Balch, M. M. Olmstead, S. P. Rowley, *Inorg. Chim. Acta* **1990**, *168*, 255–264.
[43] T. B. Rauchfuss, F. T. Patino, D. M. Roundhill, *Inorg. Chem.* **1975**, *14*, 652–656.
[44] D. Hedden, D. M. Roundhill, *Inorg. Chem.* **1985**, *24*, 4152–4158.
[45] E. Rotondo, G. Battaglia, G. Giuseppe, C. F. Priolo, *J. Organomet. Chem.* **1993**, *450*, 245–252.
[46] G. M. Sheldrick, *SHELX97* (Includes *SHELXS97* and *SHELXL97*), Release 97–2, Programs for Crystal Structure Analysis, University of Göttingen, Göttingen, Germany, **1998**.
[47] L. J. Farrugia, *J. Appl. Crystallogr.* **1999**, *32*, 837–838.

Received: May 12, 2005
Published Online: November 22, 2005

